

Sky Temperature Estimation and Measurement for Longwave Radiation Calculation

Kun Zhang¹, Timothy P. McDowell², Michaël Kummert¹

¹Polytechnique Montréal, Dept. of Mechanical Engineering, Montréal, QC, Canada

²Thermal Energy System Specialists, LLC, Madison, WI, USA

Abstract

Building Performance Simulation (BPS) tools rely on different methods to estimate the downwelling longwave radiation incident on surfaces, which can be expressed as an equivalent “effective sky temperature”. The longwave radiation is calculated using regressions based on the temperature, humidity, and cloud cover. This paper assesses the regressions implemented in 3 popular BPS tools (EnergyPlus, TRNSYS, and ESP-r) using measured data for the downwelling longwave radiation obtained from the SURFRAD network for 2 stations in Illinois and Colorado. Results show that the 3 regressions deliver acceptable estimations of the sky temperature. Differences are relatively small, with CVRMSD values in the order of 10 %. The impact on simulation results is also relatively small but not insignificant compared to other factors, especially in the context of inter-model validation exercises. The effective sky temperature is also required to model other energy systems such as unglazed solar collectors. A simulation of a PV/T collector shows that the useful thermal energy output changes by up to 11 % depending on the regression used.

Introduction

Downward longwave radiation from clouds and other constituents in the atmosphere has an impact on the heat loss of external surfaces of buildings, as well as on solar collectors (photovoltaic and thermal). In addition, the knowledge of atmospheric longwave radiation is critical in the design of radiative cooling systems (Hamberg et al. 1987; Meir et al. 2002) and water recovery systems from condensation of atmospheric water vapour (Gliha et al. 2011). In the field of climate science, knowing longwave radiation helps to forecast nocturnal frosts, fog, temperature variation and cloudiness; it is also useful for calculations on climate variability and global warming (Iziomon et al. 2003).

The concept of an effective or equivalent temperature is introduced in the domain of building simulation to describe the temperature of the atmosphere, even though it contains several layers at different temperatures. This temperature is termed Effective Sky Temperature (T_{sky}), and it provides a practical approach to approximate the infrared heat transfer from the atmosphere (“sky”). After introducing the sky temperature, the amount of longwave radiation emitting by the sky can be calculated according to the Stefan-Boltzmann law if regarding the sky as a black body.

$$\dot{Q}_{sky} = \sigma T_{sky}^4 \quad (1)$$

\dot{Q}_{sky} : atmospheric longwave radiation, W/m^2 ;

σ : Stefan-Boltzmann constant, $5.67 \times 10^{-8} W/(m^2 K^4)$;

T_{sky} : effective sky temperature, K .

A portable infrared thermometer can quickly measure the sky temperature; however, this instrument cannot give as accurate measurements as required. Researchers from other domains have designed and constructed prototype devices in the laboratory to measure the sky temperature; however, no such a device has been universally proven to give accurate measurements (Gliha et al. 2011).

Instead, the downwelling longwave radiation \dot{Q}_{sky} can be more precisely measured by a pyrgeometer or radiometer. However, due to the high cost of equipment and the challenge of instrument calibration and quality control, the measurement of longwave radiation is still rarely available (Wang & Liang 2009); for example, it is not present in Typical Meteorological Year (TMY) weather data files, such as the TMY3 (Wilcox & Marion, 2008) and CWC files (Numerical Logics, 1999), used by Building Performance Simulation (BPS) programs. Algorithms were therefore developed to estimate the sky temperature (or the downwelling longwave radiation from the sky) from other weather parameters.

Modelling longwave heat transfer from the sky

Different models have been created to approximate the atmospheric longwave radiation and the sky temperature, which can be broadly classified in two categories. The first category includes detailed methods, derived from measured profiles and properties of atmospheric constituents, such as the spectral transmittances. This method is in principle preferred; however, it suffers from the lack of fundamental information on the properties of atmospheric constituents (Berdahl & Fromberg 1981).

The second category of models is based on empirical relations (sometimes mixed with simpler physical models), where a set of regression equations are obtained to fit the experimental measurements of longwave radiation. This type of model is much more widely used and is the object of the present study. The empirical models generally introduce the concept of sky emissivity ϵ_{sky} , defined as the ratio of sky radiance to the ambient air radiance as in equation (2) (Berdahl & Fromberg 1981; Prata 1996).

$$\epsilon_{sky} = \frac{T_{sky}^4}{T_a^4} \quad (2)$$

$$T_{sky} = \epsilon_{sky}^{0.25} T_a \quad (3)$$

ϵ_{sky} : sky emissivity;

T_a : ambient dry bulb temperature, K.

Equation (3) is the transformation of equation (2). Using equations (1) and (3), the atmospheric longwave radiation is straightforward to obtain, as long as the sky emissivity is known. Thus, the problem has been converted to finding an algorithm for the sky emissivity.

Sky emissivity

The algorithm for the sky emissivity can be generally divided into two steps: first calculating the emissivity ε_{clear} under clear sky conditions; then applying a cloud cover correction to get the all sky emissivity ε_{sky} .

The literature includes three main approaches to calculate the clear sky emissivity. The first approach is based on the ambient temperature, as proposed by (Swinbank 1963). One of the representative equations is given below.

$$\varepsilon_{clear} = 5.31 \times 10^{-13} T_a^2 \quad (4)$$

This approach has been shown to result in larger deviations than others (Wang & Liang 2009; Flerchinger et al. 2009).

The second approach is based on water vapour pressure. Although not adopted in the domain of building simulation, this type of regression is widely studied in other disciplines such as meteorology. A common form of the empirical regression with water vapour pressure can be written as follows.

$$\varepsilon_{clear} = \alpha_1 + \beta_1 P_v^\gamma \quad (5)$$

P_v : water vapour pressure;

$\alpha_1, \beta_1, \gamma$ are the coefficients of the equation. Different researchers proposed different coefficients in the past to fit measurements from different regions and time periods (Flerchinger et al. 2009).

The advantage of this formula is its simplicity with only one variable. The water vapour pressure can for example be calculated using the relative humidity and the saturation pressure of water at the ambient temperature.

The last approach is based on dew point temperature. This is the common practice approach in BPS software programs. This type of regression will be discussed in detail in the next section.

After obtaining the clear sky emissivity, a cloud cover correction needs to be applied to get the full sky equation. A method to estimate the cloudiness c is using a clarity index, defined as the ratio of total solar radiation to extraterrestrial radiation (or sometimes to estimated clear sky radiation). The cloudiness can then be linearly interpolated between 0 and 1 with the clarity index. Other relations between cloud cover and solar radiation have also been proposed (Flerchinger et al. 2009). However, this cloudiness factor is not necessarily related to the data of opaque and total sky cover recorded in the TMY weather file used in the building simulation.

The cloudiness c is then used to correct the clear sky emissivity. Different correction equations were proposed

by different researchers, most of which have the following form:

$$\varepsilon_{sky} = \varepsilon_{clear}(1 + \alpha_2 c^{\beta_2}) \quad (6)$$

α_2, β_2 are the coefficients.

Algorithms in BPS programs

There are two major algorithms adopted in BPS programs, one based on the work of (Clark & Allen 1978), the other (Martin & Berdahl 1984; Berdahl & Martin 1984). As discussed previously, dew point temperature is used to calculate the clear sky emissivity in these two algorithms. The cloud correction is normally calculated using sky cover data available in TMY and other standard weather data files. If cloud cover data are not available, programs typically include methods to estimate the cloud cover from solar radiation (and extrapolate these values at night), but these methods are not discussed in the present paper.

This paper focuses on the models integrated in three popular BPS programs, respectively EnergyPlus (US DOE 2016), TRNSYS (Klein et al. 2014), and ESP-r (ESRU 2002). EnergyPlus utilizes the Clark-Allen method, while TRNSYS and ESP-r use slightly different variants of the Martin-Berdahl algorithm. ESP-r offers different options to calculate longwave radiation from the sky but this paper only considers the default method.

Martin-Berdahl Model

After conducting a program of sky radiance measurement in six different U.S. cities, Martin-Berdahl proposed a quadratic relation between the monthly average clear sky emissivity and the monthly average dew point temperature ($^{\circ}\text{C}$) as shown in equation (7).

$$\varepsilon_m = 0.711 + 0.56 \left(\frac{T_{dp}}{100} \right) + 0.73 \left(\frac{T_{dp}}{100} \right)^2 \quad (7)$$

ε_m is monthly average clear sky emissivity. The range of the monthly average dew point temperature T_{dp} was from -13°C to 24°C . In order to predict hourly clear sky emissivity, an approximate diurnal correction ε_h is added to the monthly average emissivity ε_m .

$$\varepsilon_h = 0.013 \cos \left(2\pi \frac{t}{24} \right) \quad (8)$$

t is the hour of the day. An additional elevation correction ε_e is added to adjust for the pressure difference in different elevations of the observing stations.

$$\varepsilon_e = 0.00012 (P - 1000) \quad (9)$$

P is the station pressure in millibars. Therefore, the hourly clear sky emissivity is written as:

$$\varepsilon_{clear} = \varepsilon_m + \varepsilon_h + \varepsilon_e \quad (10)$$

Then a relationship between the clear sky emissivity and cloudy sky emissivity is proposed by introduction of the “infrared cloud amount” C .

$$\varepsilon_{sky} = \varepsilon_{clear} + (1 - \varepsilon_{clear})C \quad (11)$$

$$C = n\varepsilon_c \Gamma \quad (12)$$

n is the fractional area of the sky covered by clouds (cloud cover fraction, between 0 and 1); ε_c is the cloud emissivity and Γ is a factor depending on the cloud base temperature. When the cloud fraction n is 0, i.e., the sky is clear, the infrared cloud amount C is also 0; in this case, the sky emissivity equals clear sky emissivity. When the infrared cloud amount C is close to 1, the sky emissivity is also close to 1; in this situation, the sky temperature is close to the ambient temperature.

Due to difficulty of obtaining accurate measurement of the cloud factor Γ , an approximation is proposed by assuming a fixed lapse rate of cloud base temperature equal to 5.6 °C/km, resulting in equation (13).

$$\Gamma = e^{-\frac{h}{h_0}} \quad (13)$$

h is the cloud base height and h_0 equals 8.2 km. As stated in the paper, “The lapse rates in the first kilometer above the earth’s surface vary from 3.5 °C/km for the mid-latitude winter atmosphere to 6.5 °C/km for the U.S. standard atmosphere”. A linear superposition can be made in equation (12) to calculate the total infrared cloud amount C if there are different layers of clouds (with different cloud fractions, emissivities and cloud factors).

The cloud base temperature factor Γ cannot be easily derived from weather data which is typically available, so a simpler estimate of C is provided in (Martin & Berdahl 1984).

$$C = C_{thin} + C_{opaque} \quad (14)$$

C_{thin} and C_{opaque} are defined as:

$$C_{thin} = n_{thin} \varepsilon_{thin} e^{-h_{thin}/h_0} \quad (15)$$

$$C_{opaque} = n_{opaque} \varepsilon_{opaque} e^{-h_{opaque}/h_0} \quad (16)$$

with n_{thin} and n_{opaque} respectively as the fractional area of the sky covered with thin and opaque clouds, ε_{thin} and ε_{opaque} respectively the thin and opaque cloud emissivity, and h_{thin} and h_{opaque} respectively the thin and opaque cloud base height. h_0 is 8.2 km, as in equation (13).

Often, the fractional area of the sky covered by total and opaque clouds (n_{total} and n_{opaque}) are available, so n_{thin} is estimated as:

$$n_{thin} = n_{total} - n_{opaque} \quad (17)$$

Estimated (constant) values can be used for the cloud emissivities ($\varepsilon_{thin} = 0.4$; $\varepsilon_{opaque} = 1.0$) and for the thin and opaque cloud base height ($h_{thin} = 8$ km, $h_{opaque} = 2$ km). If the entire cloud cover is opaque ($n_{total} = n_{opaque}$), the simplified expression for C is reduced to:

$$C = n_{opaque} \cdot 0.784 \quad (18)$$

Clark-Allen (EnergyPlus) model

Using one-year measurements in San Antonio, Texas from 1976 to 1977, Clark-Allen proposed a logarithmic regression between the clear sky emissivity and dew point temperature as in equation (19).

$$\varepsilon_{clear} = 0.787 + 0.7641 \ln \left(\frac{T_{dp}}{273} \right) \quad (19)$$

T_{dp} is the dew point temperature in Kelvin. The dew point temperature range in their study was from -20 °C to 25 °C, which corresponded to a range of water vapor pressure from 3 to 25 millibars. Then a cloud correction factor C_a was adopted to correct the sky emissivity for cloudy circumstances.

$$\varepsilon_{sky} = \varepsilon_{clear} C_a \quad (20)$$

$$C_a = 1 + 0.0224n - 0.0035n^2 + 0.00028n^3 \quad (21)$$

n is the opaque sky cover in tenths ($0 \leq n \leq 10$), which is available in typical weather data files such as the EPW format. Equation (21) shows that when the opaque sky cover is 0, the cloud correction factor is 1, which coincides with equation (19). Clark and Allen report that the standard estimation error for the atmospheric longwave radiation was 10 W/m².

Implementation in TRNSYS

The sky temperature model in TRNSYS Type 15 (weather data reader and processor) uses the Martin-Berdahl method with the simplification that C is estimated with a simple expression:

$$C = n_{opaque} \cdot 0.9 \quad (22)$$

The origin of the 0.9 factor is unclear; it could have been selected slightly higher than the value in equation (18) to compensate for the fact that the impact of thin clouds is neglected.

When cloud cover is not available, e.g. for the German TRY weather data format, the following equations are used to calculate the cloud fraction f_{cloud} .

$$f_{cloud} = \left(1.4286 \frac{E_{dif}}{E_{glob,h}} - 0.3 \right)^{0.5} \quad (23)$$

$$E_{glob,h} = E_{dir} + E_{dif} \quad (24)$$

E_{dif} : diffuse radiation on the horizontal

E_{dir} : beam radiation on the horizontal

$E_{glob,h}$: total radiation on the horizontal

For the night cloud fraction ($E_{glob,h} = 0$), an averaged value over the afternoon is used. All our comparisons include cloud cover data so this estimation has not been used in the present paper.

ESP-r model

The default method to estimate longwave radiation from the sky in ESP-r is the Martin-Berdahl method presented in equations (7)~(10) to calculate the clear sky emissivity ε_{clear} . The “infrared cloud amount” C is calculated using the fractional area of the sky covered by clouds n as an input:

$$C = n \Gamma \quad (25)$$

$$\Gamma = e^{-h/h_0} \quad (26)$$

The difference with TRNSYS is that the equations above are used directly, assuming $n = n_{opaque}$ and $h = 3$ km ($h_0 = 8.2$ km as in the original reference), which gives:

$$C = n_{opaque} \cdot 0.694 \quad (27)$$

Comparing equations (27) and (22), this leads to a reduced impact of cloud cover on the calculated sky emissivity.

ESP-r users can optionally select five other regressions to estimate the sky temperature. A preliminary comparison showed that these additional methods did not give significantly better estimations than the default one so they were not considered for further analysis.

Methodology

The objective of this paper is to assess the differences between the 3 methods implemented in EnergyPlus, TRNSYS, and ESP-r to estimate longwave radiation from the sky. The differences between estimated values will be assessed and all results will also be compared to measured values for selected locations and time periods.

The impact of these differences on simulation results will also be assessed by calculating building thermal loads of a simple test cell and of an office building and by calculating the electrical and thermal performance of a Photovoltaic/Thermal (PV/T) collector used for fresh air preheating.

Two procedures were conducted for the evaluation work. The first step was calculating the sky temperature and longwave radiation based on the algorithms adopted in the programs, using the measured weather data. Then we compared the calculated results of longwave radiation with the measured. Different statistics were used to assess the goodness of fit of the different methods and between the methods.

The second step was running the simulations with both the calculated and “measured” sky temperature for different building cases and solar collectors, assessing peak and annual loads.

All algorithms were re-coded by the authors in a pre-processing phase, and the estimated sky temperature was then read-in directly in TRNSYS for all simulations. The short names used to distinguish the 3 regressions (EnergyPlus, TRNSYS, ESP-r) refer to the BPS tools that use that particular method. However, it should be noted that this paper does not present a comparison between simulation results obtained with the different programs, but rather a comparison between TRNSYS results obtained using 3 different sky temperature estimation methods. This methodology was selected to isolate the impact of using different sky temperature estimates from other differences introduced by using different algorithms for different part of the building/system models.

Data sources

The measured data for longwave radiation was obtained from the Surface Radiation Budget Network (SURFRAD) at (National Oceanic and Atmospheric Administration, 2016). Downwelling longwave radiation (also known as infrared thermal radiation) from the clouds and other atmospheric constituents is measured by an upward facing pyrgeometer.

SURFRAD pyrgeometers are recalibrated annually against standard instruments whose calibrations are traceable to the world standard in Davos, Switzerland. The SURFRAD website indicates that 90 % of the measurements are within 11 W/m², and 99 % are within 15 W/m² of the standards. Current accuracy achievable for pyrgeometers is in the order of 5 W/m², but we have chosen to use a ± 15 W/m² margin to represent the uncertainty on SURFRAD measurements covering the 1995-2012 period.

Cloud cover, which is used by all sky temperature regressions, is not directly available in SURFRAD data. Therefore, additional weather data from close-by weather stations (generally airports) was used in this study.

The two SURFRAD stations selected for the longwave radiation data were Boulder, CO (hereafter referred to “Colorado” or “CO”) and Bondville, IL (hereafter referred to as “Illinois” or “IL”) to represent different climates and elevations. For these two stations, there are two weather stations nearby: Vance-Brand-AP, Colorado (located approximately 8 km away from the SURFRAD station) and University of Illinois, Illinois (located approximately 6.5 km away from the SURFRAD station). Comparisons for parameters measured at SURFRAD stations and also available at airports (e.g. dry bulb temperature and humidity) showed an excellent agreement between the different data sources.

The year 2012 for the two weather stations were chosen based on the quality of airport weather data and availability of longwave radiation measurements. Airport weather data was procured from WhiteBox Technologies (WhiteBox Technologies, 2016) for the year 2012 for both airport stations. It was observed that the EPW files obtained from WhiteBox Technologies contain identical data for opaque sky cover and total sky cover.

A TMY3 weather file (Wilcox & Marion, 2008) is also available for the University of Illinois, IL station. That composite file contains individual months from selected years between 1995 and 2004, for which SURFRAD data is also available. The data includes different values for the opaque and total sky cover. The different sky temperature regressions were also compared using the individual months in the TMY3 data to assess the impact of neglecting the difference between total and opaque sky cover.

Data processing

The longwave radiation measurements recorded by the SURFRAD stations are mean values over 3 minute or 1 minute depending on the measurement period. This raw data was averaged over 1 hour to allow a direct comparison with other data sources (White Box Technologies and TMY3). Instantaneous hourly values in these data sources (e.g. dry bulb temperature) were also averaged over the hour by taking the arithmetic mean of two successive values.

Missing data in the SURFRAD data files were replaced with NaN values in the data processing. When deriving

hourly values, hours with up to 12 min of missing data were calculated from the available sub-hourly (3-min or 1-min) time steps, while hours with more than 12 min missing were set to NaN. These hours are not included in the aggregated (e.g. yearly) comparison indices. Less than 1 % of the hourly time steps are missing in the 2012 comparisons, and 3 % of the hourly time steps are missing in the TMY3 data. When performing TRNSYS simulations using the measured downwelling longwave radiation, missing values were set to a value obtained by averaging the 3 compared regressions.

Results

Goodness of fit statistics

This section defines the different statistics used in the results analysis. In the following equations, y denotes the calculated value (e.g. \dot{Q}_{sky} obtained from the different regressions), and y_m denotes the measured value.

The Root Mean Squared Error (RMSE) is an absolute value in the variable units (e.g. W/m² for \dot{Q}_{sky}):

$$RMSE = \sqrt{\sum \frac{(y - y_m)^2}{N}} \quad (28)$$

The RMSE can be normalized by dividing it by the average value of the measured variable, and expressed in %. This is usually referred to as the Coefficient of Variation of the RMSE (CVRMSE):

$$CVRMSE = \frac{\sqrt{\sum \frac{(y - y_m)^2}{N}}}{\bar{y}_m} \times 100\% \quad (29)$$

The RMSE is an unsigned value, so it does not indicate whether a model has a bias error. The Mean Bias Error can be used for that purpose. It is again a value expressed in the same units as the variable:

$$MBE = \frac{\sum (y - y_m)}{N} \quad (30)$$

The MBE can be normalized by dividing the value by the average of measured values, as for the CVRMSE. This gives the Normalized Mean Bias Error (NBME), expressed in %:

$$NBME = \frac{\sum (y - y_m)}{\bar{y}_m} \times 100\% \quad (31)$$

Finally, the maximum absolute error (AE_{max}) and its normalized version (NAE_{max}) are simply defined as:

$$AE_{max} = \max(|y - y_m|) \quad (32)$$

$$NAE_{max} = \frac{\max(|y - y_m|)}{\bar{y}_m} \times 100\% \quad (33)$$

These statistics can also be used to assess the differences between two models, when no truth standard exists. In that case the term ‘‘Difference’’ is used instead of ‘‘Error’’, e.g. RMSD for Root Mean Squared Difference.

Calculated downwelling longwave radiation

Table 1 (see end of paper) shows the goodness of fit statistics for the 3 regressions vs. measured values, as well as between the regressions. The 3 datasets are assessed independently and then a 4th value is computed

by combining all hourly values in one single data set, which includes the year 2012 and the composite TMY3 year for Bondville, IL and the year 2012 for Boulder, CO.

The *RMSE* and *CVRMSE* values show that the 3 regressions are relatively similar, with *RMSE* values in the order of 20 to 30 W/m², or *CVRMSE* of 6 to 10 %. These values indicate a relatively good fit, as the *RMSE* is less than twice the estimated measurement uncertainty (15 W/m²). The Colorado station shows higher errors, and the EnergyPlus regression performs slightly better for that station, while it is slightly worse than the other regressions for the Illinois station. The climate at the two stations is very different, with the Colorado being at higher altitude (1540 m vs. 210 m), dryer (average water vapour pressure of 0.6 kPa vs. 1.2 kPa) and less cloudy (average cloud cover of 2 vs. 3 and 5 for the different periods). The small differences and the limited dataset do not allow to draw general conclusions.

The *MBE* values reveal interesting differences: the regressions based on the Martin-Berdahl algorithm tend to underestimate \dot{Q}_{sky} (i.e. overestimate radiative losses to the sky), while the EnergyPlus regression (based on Clark and Allen) tends to overestimate \dot{Q}_{sky} . Again, the differences are small, with *NBME* in the order of +/- 5 %. For the Colorado station, the differences between the two categories of regressions are more pronounced with differences about 10 % between the TRNSYS and EnergyPlus (or ESP-r and EnergyPlus) regressions. This would result in radiative losses from a horizontal surface being lower using the EnergyPlus regression than using the TRNSYS or ESP-r regressions. Maximum absolute errors are higher, with hourly values up to 120 W/m² or 40 % of the average value of \dot{Q}_{sky} , which is around 300 W/m² for both stations. These values occur for relatively short periods, as discussed below.

Figure 1 shows a scatter plot of the error on \dot{Q}_{sky} for all datasets and the 3 regressions vs. the opaque cloud cover. The grey area represents a +/- 15 W/m² uncertainty range for measurements. The scatter plot is much denser in that area, but errors in the order of 50 W/m² are relatively frequent. The best linear fit lines reveal that the EnergyPlus regression tends to overestimate \dot{Q}_{sky} for low cloud cover values and underestimate \dot{Q}_{sky} at high cloud cover values, while the other regressions have an opposite behaviour. The ESP-r regression generally results in values lower than the ones obtained from the TRNSYS regression.

Figure 2 presents the modelled and measured longwave radiation for five typical winter days in Colorado (top) and Illinois (bottom). The measured values are again represented with a ± 15 W/m² uncertainty. The plots also show the opaque sky cover in percent. The sky cover is the main driver of quick changes in \dot{Q}_{sky} , which is also influenced by the humidity and ambient temperature.

During the selected days, the TRNSYS regression seems to capture the amplitude of longwave radiation

oscillations better than the EnergyPlus regression, while the ESP-r regression sometimes coincides with TRNSYS and sometimes with EnergyPlus. The TRNSYS regression is also the one that shows the largest errors over specific periods. Given that the overall goodness of fit (see above) is similar (or slightly worse than the EnergyPlus regression for Colorado), this would seem to indicate that the TRNSYS regression is often closer to the measured value than the others, but also presents the largest short-term errors. In particular, the TRNSYS regression seems to show the strongest response to changes in cloudiness levels, sometimes overestimating their impact.

Comparison of building thermal loads

Three simulations were performed to assess the impact of using different estimations for the sky temperature (hence the downwelling longwave radiation). In all cases, the weather data file for the Colorado station (2012) was used, as it resulted in the largest discrepancies between the different algorithms. As described in the methodology, all simulations are run in TRNSYS using pre-processed values with the results of the 3 compared regressions (TRNSYS allows to disconnect most of its inputs from their “normal” connections and instead use values calculated by equations or read from an input file).

The first simulation is one of the test cases in the building envelope validation tests provided by ASHRAE standard 140: *Standard Method of Test for the Evaluation of Building Energy Analysis Computer Programs* (ASHRAE, 2014). The selected case is the initial low-mas Case 600. Readers should note that the Test Case description we used is taken from the current draft of the document, which is being updated. The weather file is also different from the one used in the standard, although both locations are in Colorado. For this reason, the absolute values of the results presented below cannot be directly compared with results published in the standard.

Table 2 (see end of paper) summarizes the differences of thermal loads from the programs against the measurements for Case 600. We can see that the differences between the regressions and the measured value and between the different regressions are consistent with the observations in the previous section. The EnergyPlus regression shows a better fit of measured values for that location, hence the calculated loads are closer to the ones obtained with the measurements. Compared to the TRNSYS regression, the EnergyPlus regression estimates a higher downwelling longwave radiation, which results in increased cooling loads and reduced heating loads. The impact on peak hourly values is slightly lower but in the same direction (i.e. less heating for EnergyPlus).

The order of magnitude of the differences in annual loads between the EnergyPlus and TRNSYS regressions is relatively small, between 6 and 7 %. But this order of magnitude is similar to the differences observed in intermodel comparison (i.e. comparing the EnergyPlus

program with the TRNSYS program). For that particular test case (Case 600) and the particular weather file used, this means that the relative difference between the two programs would go down from 5 % to ≈ 1 % simply by changing the sky temperature regression used in TRNSYS. This makes the case for better assessing and documenting the estimation methods used by the different programs involved in inter-model validation exercises.

Another simulation was run with the upper floor of a large office building adapted from DOE’s commercial building database “large office” example. The last (upper) floor was selected because it is located under the roof, hence being more sensitive to the radiative heat balance of the roof. *Table 3* summarizes the thermal loads for the office building using the weather data Boulder, CO in 2012. Comparing with *Table 2*, the differences are smaller than for Case 600, which can be attributed to the higher importance of internal and solar gains. But the same trends are observed.

Comparison of PV/T collector performance

A PV/T collector used for fresh air preheating is modeled in TRNSYS using Type 569. The parameters (including the air flowrate, rated efficiencies and other parameters) are taken from (Delisle & Kummert 2016). The fan is assumed to operate only when the potential for heat gain is there, which is assessed by a outlet – inlet temperature difference greater than 5 °C.

Table 4 shows the annual and peak heat gain obtained with the 3 regressions and with measured data. Peak values are relatively unaffected, but the EnergyPlus regression leads to a 11 % increase in the thermal output compared to using measured values of \dot{Q}_{sky} . The difference with results obtained using the TRNSYS regression is in the order of 7 %. The electrical output does not show significant differences.

Conclusions

This paper discussed different models to estimate downward longwave radiation. The regressions used to derive an “effective sky temperature” in EnergyPlus, TRNSYS, and ESP-r were compared to measured data obtained from the SURFRAD network. Two stations were selected (Bondville, IL and Boulder, CO) and 3 years of data were used in total (full 2012 year for both stations, and composite TMY3 year for Bondville, IL). The 3 regressions provide acceptable estimates for the downwelling longwave radiation from the sky, with annual CVMSE values below 10 %. Larger errors occur over short periods. The ESP-r and TRNSYS regressions share the same basis (Martin and Berdahl correlation), while the EnergyPlus regression is based on another approach (Clark and Allen). This leads to the ESP-r and TRNSYS regressions results being closer to each other than to the EnergyPlus results.

The 3 regressions have non-zero Mean Bias Errors. The differences between regressions can be larger than the difference between any of them and the measured values. Data from the Colorado station leads to the

largest differences, with Normalized Mean Bias Differences between the EnergyPlus and TRNSYS regressions in the order of 10 %. The EnergyPlus regression tends to result in a higher downwelling longwave radiation.

Simulation comparisons were performed in TRNSYS using pre-processed sky temperature values calculated with the different regressions. The results confirm that the EnergyPlus regression leads to reduced heating loads and increased cooling loads due to the higher longwave radiation from the sky. The differences for Case 600 of ASHRAE Standard 140 are in the same order of magnitude as the differences obtained from different simulation engines (EnergyPlus vs. TRNSYS). This means that the different sky temperature regressions could account for a significant part of the discrepancies obtained in inter-model validation exercises. Differences as high as 7 % for annual heating and cooling were found in Case 600. The upper floor of a large office building was simulated as well, showing slightly smaller differences (in the order of 5 %) with the same trends. Finally, a simulation of an unglazed PV/T collector showed differences up to 11 % in the useful annual thermal energy output, with negligible differences in electrical output.

This work shows that the different methods used to estimate downwelling longwave radiation in BPS tools can lead to differences in results that are significant in the context of inter-model validation exercises or for specific systems sensitive to longwave radiation, such as unglazed solar collectors. Further work should aim at developing more accurate regressions and implement them in BPS tools.

References

- ASHRAE. ANSI/ASHRAE Standard 140-2014 – Standard Method of Test for the Evaluation of Building Energy Analysis Computer Programs. Atlanta, GA, USA: American Society of Heating, Refrigerating and Air-conditioning Engineers; 2014.
- Berdahl, P. & Fromberg, R., 1981. *An empirical method for estimating the thermal radiance of clear skies*, Berkeley, CA, USA.
- Berdahl, P. & Martin, M., 1984. Emissivity of Clear Skies. *Solar Energy*, 32(5), pp.663–664.
- Clark, G. & Allen, C., 1978. The Estimation of Atmospheric Radiation for Clear and Cloudy Skies. In *Proceedings of the 2nd National Passive Solar Conference*. pp. 675–678.
- Delisle, V. & Kummert, M., 2016. Cost-benefit analysis of integrating BIPV-T air systems into energy-efficient homes. *Solar Energy*, 136, pp.385–400.
- ESRU. 2002. *The ESP-r system for building energy simulation, User guide Version 10 series*. Glasgow: University of Strathclyde, Energy Systems Research Unit.
- Flerchinger, G.N. et al., 2009. Comparison of algorithms for incoming atmospheric long-wave radiation. *Water Resources Research*, 45(3), pp.1-13.
- Glihah, O. et al., 2011. The effective sky temperature: An enigmatic concept. *Heat and Mass Transfer/Waerme- und Stoffuebertragung*, 47(9), pp.1171–1180.
- Hamberg, I. et al., 1987. Radiative cooling and frost formation on surfaces with different thermal emittance: theoretical analysis and practical experience. *Applied optics*, 26(11), pp.2131–2136.
- Iziomon, M.G., Mayer, H. & Matzarakis, A., 2003. Downward atmospheric longwave irradiance under clear and cloudy skies: Measurement and parameterization. *Journal of Atmospheric and Solar-Terrestrial Physics*, 65(10), pp.1107–1116.
- Klein, S. A., et al. 2014. *TRNSYS 17 – A TRaNsient SYstem Simulation program, User manual. Version 17.2.5*. Madison, WI: University of Wisconsin-Madison.
- Martin, M. & Berdahl, P., 1984. Characteristics of Infrared Sky Radiation in The US. *Solar Energy*, 33(3/4), pp.321–336.
- Meir, M.G., Rekstad, J.B. & LØVVIK, O.M., 2002. A study of a polymer-based radiative cooling system. *Solar Energy*, 73(6), pp.403–417.
- National Oceanic and Atmospheric Administration., 2016. Available from: <http://www.esrl.noaa.gov/gmd/grad/surfrad/index.html>. [12 December 2016].
- Numerical Logics. Canadian weather for energy calculations, user's manual and CD-ROM. Downsview, ON, Canada: Environment Canada; 1999.
- Prata, A.J., 1996. A new long-wave formula for estimating downward clear-sky radiation at the surface. *Quarterly Journal of the Royal Meteorological Society*, 122(533), pp.1127–1151.
- Swinbank, W.C., 1963. Long-wave radiation from clear skies. *Quarterly Journal of the Royal Meteorological Society*, 89(381), pp.339–348.
- US DOE .2016. *EnergyPlus engineering reference - The reference to EnergyPlus calculations (v 8.5)*. Washington, DC, USA: US Department of Energy.
- Wang, K. & Liang, S., 2009. Global atmospheric downward longwave radiation over land surface under all-sky conditions from 1973 to 2008. *Journal of Geophysical Research*, 114(D19), pp.1–12.
- WhiteBox Technologies., 2016. Available from: <http://weather.whiteboxtechnologies.com/>. [12 December 2016].
- Wilcox S, Marion W. Users manual for TMY3 data sets., 2008. 58 pp.; *National Renewable Energy Laboratory, Golden, CO, USA: NREL Report No. TP-581-43156*; National Renewable Energy Laboratory, Golden, CO, USA.

Table 1: Goodness of fit statistics for \dot{Q}_{sky}

State	Period	EnergyPlus vs. Measured	TRNSYS vs. Measured	ESP-r vs. Measured	EnergyPlus vs. TRNSYS	EnergyPlus vs. ESP-r	TRNSYS vs. ESP-r
RMSE (or RMSD) [W/m²]							
Illinois	TMY3	24.4	24.0	23.1	17.1	13.0	11.8
Illinois	2012	20.0	19.8	19.4	18.9	16.6	9.8
Colorado	2012	26.8	30.2	28.9	33.4	33.0	8.6
All sets	combined	23.9	25.1	24.1	24.3	22.6	10.2
CVRMSE (or CVRMSD) [%]							
Illinois	TMY3	7.6	7.5	7.2	5.4	4.1	3.7
Illinois	2012	6.2	6.1	6.0	5.9	5.1	3.0
Colorado	2012	9.2	10.4	9.9	11.5	11.3	3.0
All sets	combined	7.7	8.1	7.8	7.8	7.3	3.3
MBE (or MBD) [W/m²]							
Illinois	TMY3	3.0	6.1	-3.1	-3.1	6.0	9.1
Illinois	2012	2.4	-2.0	-8.0	4.5	10.4	6.0
Colorado	2012	11.6	-13.1	-17.4	24.7	29.0	4.3
All sets	combined	5.7	-3.1	-9.5	8.7	15.1	6.4
NMBE (or NMBD) [%]							
Illinois	TMY3	1.0	1.9	-1.0	-1.0	1.9	2.8
Illinois	2012	0.7	-0.6	-2.5	1.4	3.2	1.9
Colorado	2012	4.0	-4.5	-6.0	8.5	9.9	1.5
All sets	combined	1.8	-1.0	-3.1	2.8	4.9	2.1
AE_{max} (or AD_{max}) [W/m²]							
Illinois	TMY3	108.2	124.0	106.6	39.6	39.6	24.6
Illinois	2012	65.6	90.3	91.4	44.2	44.2	25.3
Colorado	2012	108.5	114.9	114.7	60.7	60.7	29.1
All sets	combined	108.5	124.0	114.7	60.7	60.7	29.1
NAE_{max} (or NAD_{max}) [%]							
Illinois	TMY3	33.9	38.8	33.4	12.4	12.4	7.7
Illinois	2012	20.3	28.0	28.3	13.7	13.7	7.8
Colorado	2012	37.3	39.5	39.4	20.8	20.8	10.0
All sets	combined	34.9	39.9	36.9	19.5	19.5	9.4

Table 2: Thermal load differences for Boulder, CO in 2012 (Case 600)

	Peak heating Ph (kW)	Difference Ph (%)	Annual heating Qh (kWh)	Difference Qh (%)	Peak cooling Pc (kW)	Difference Pc (%)	Annual cooling Qc (kWh)	Difference Qc (%)
Measured	3.40	0	4356	0	6.19	0	6638	0
EnergyPlus	3.46	1.6	4341	-0.4	6.42	3.7	6893	3.8
TRNSYS	3.62	6.5	4663	7.0	6.17	-0.2	6518	-1.8
ESP-r	3.62	6.5	4735	8.7	6.17	-0.3	6486	-2.3

Table 3: Thermal load differences for Boulder, CO in 2012 (Office building)

	Peak heating Ph (kW)	Difference Ph (%)	Annual heating Qh (MWh)	Difference Qh (%)	Peak cooling Pc (kW)	Difference Pc (%)	Annual cooling Qc (MWh)	Difference Qc (%)
Measured	220.5	0	115.4	0	325.7	0	177.8	0
EnergyPlus	220.4	-0.1	114.4	-1.1	327.1	0.4	182.2	2.5
TRNSYS	222.3	0.8	119.0	3.1	322.5	-1.0	174.9	-1.6
ESP-r	222.4	0.9	120.1	4.1	322.3	-1.1	174.0	-2.1

Table 4: Useful heat gain from PV/T module for Boulder, CO in 2012

	Peak heat Ph (kW)	Difference Ph (%)	Annual heat Qh (kWh)	Difference Qh (%)
Measured	23.45	0	29764	0
EnergyPlus	23.54	0.35	33032	11.0
TRNSYS	23.50	0.19	30841	3.6
ESP-r	23.19	-1.14	30517	2.5

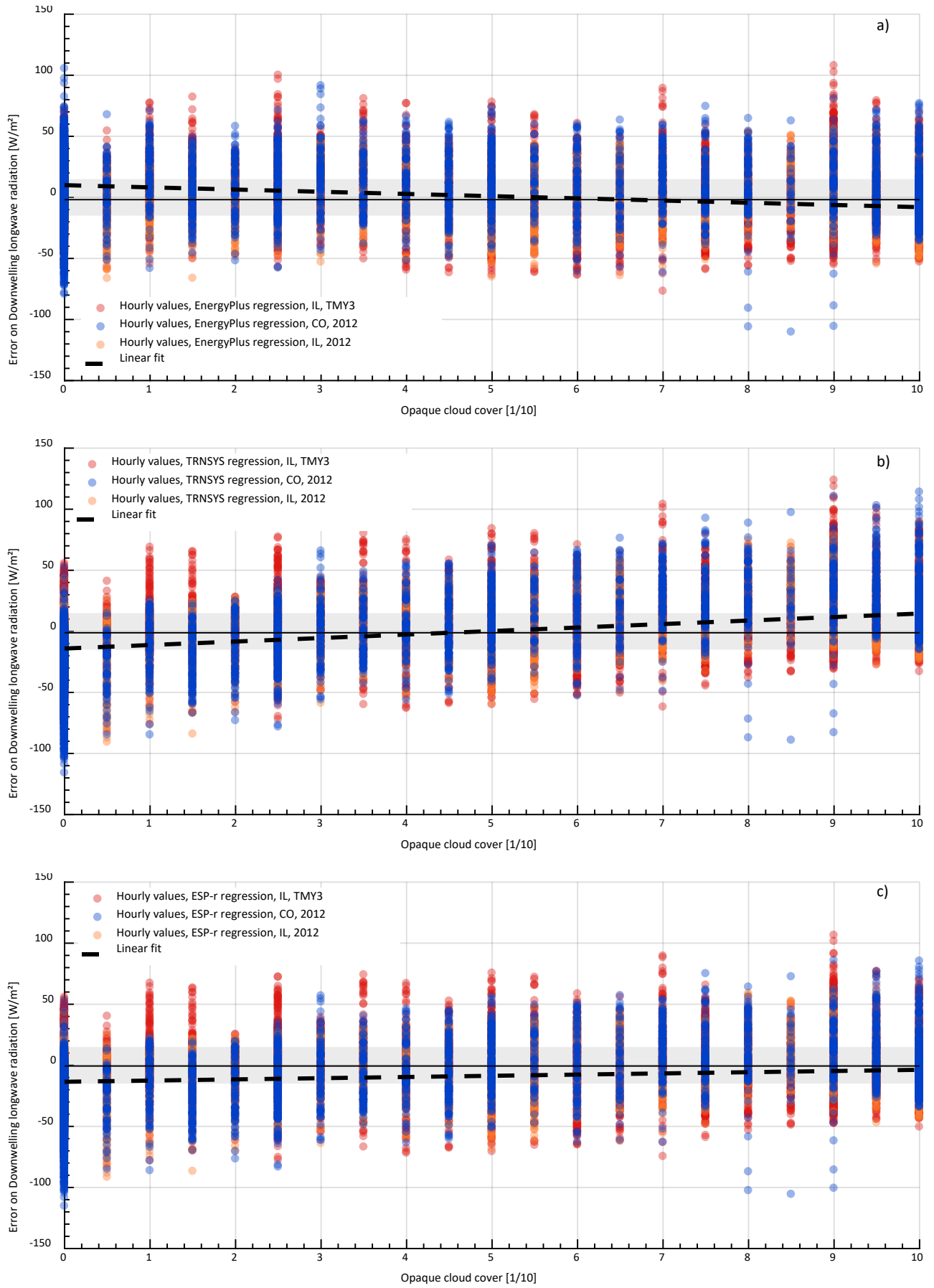


Figure 1: Scatter plot of calculated \dot{Q}_{sky} vs. opaque sky cover, EnergyPlus (a), TRNSYS (b) and ESP-r (c) regressions

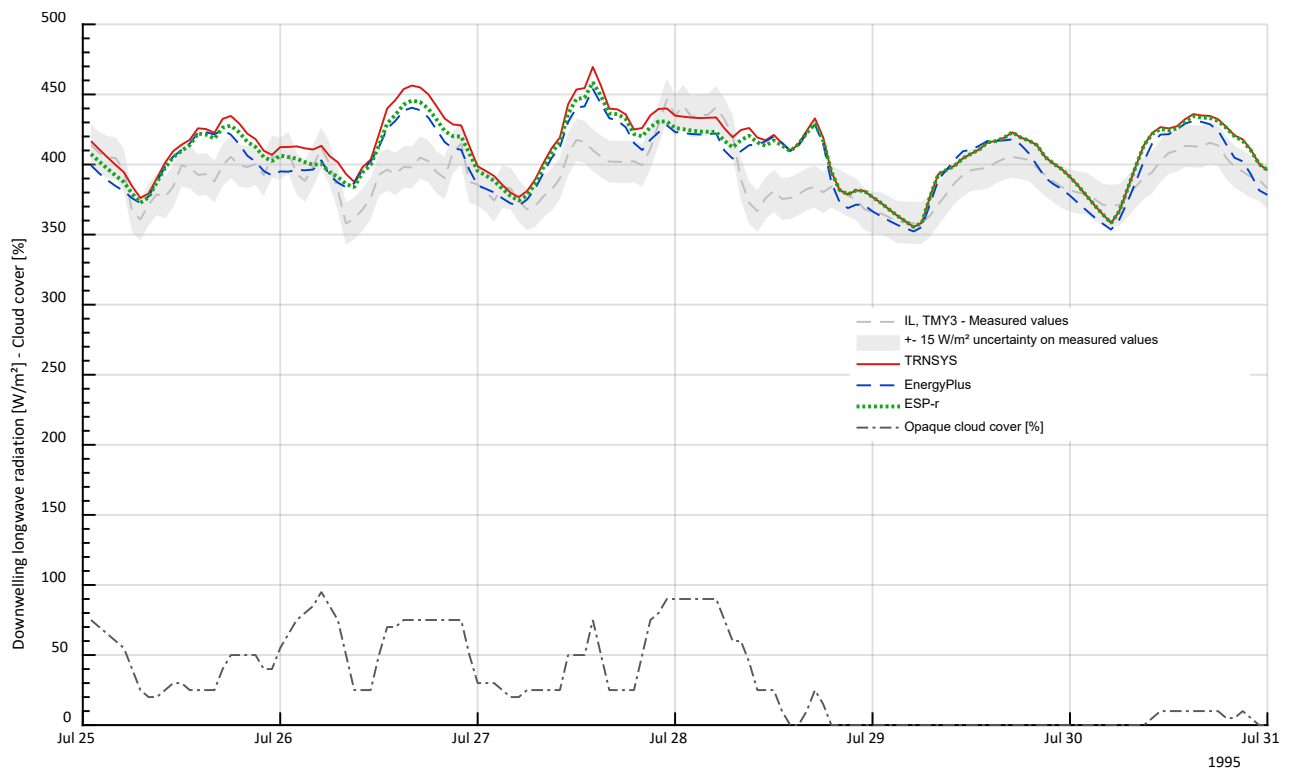
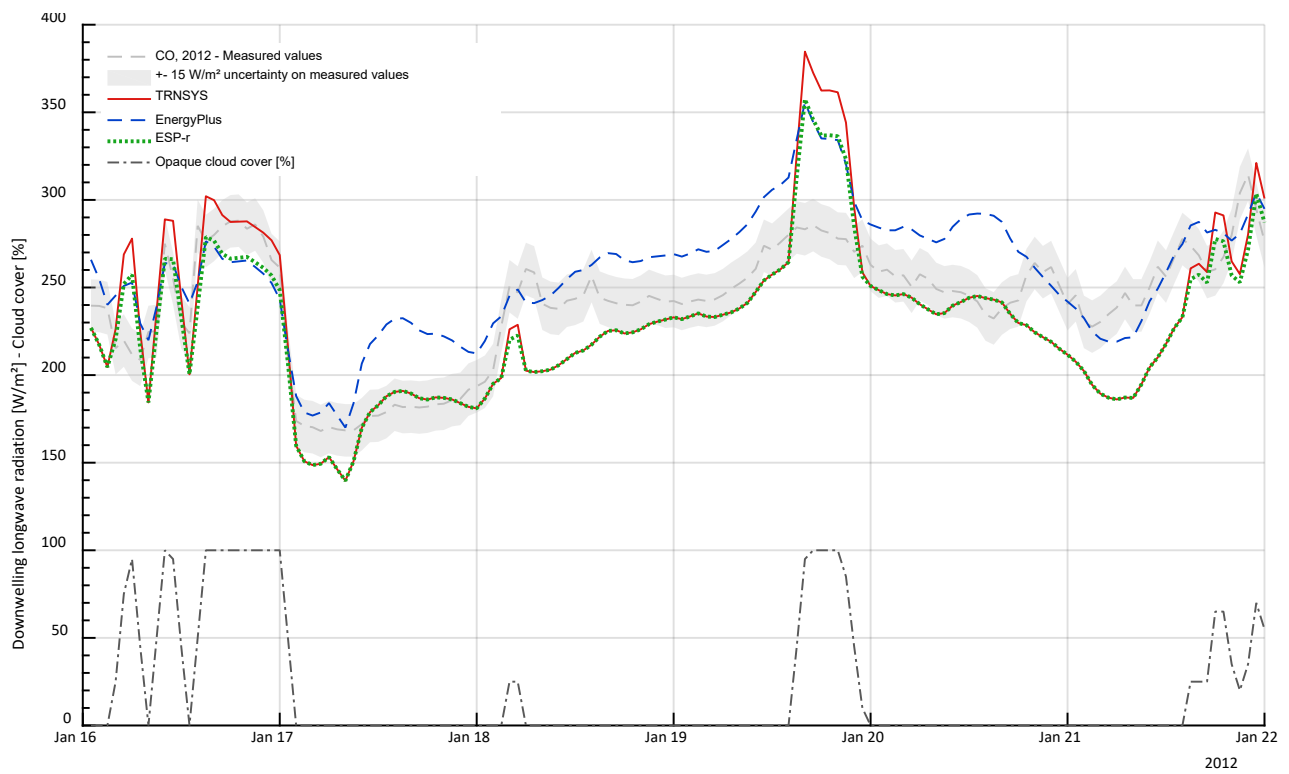


Figure 2: Comparison of measurements and estimations of longwave radiation for selected days in January, Colorado 2012 (top) and July, Illinois 1995 (bottom)